remote sensing

MDPI

Supplementary Materials

Table 1. All the recorded earthquakes by USGS in the study area from 2009 to Sep. 2019 [1].

Time	Latitude	Longitude	Depth	Mag.	MagType
2009-10-13T00:54:28.000Z	34.88	46.85	13	4.8	mwc
2011-04-06T19:17:17.500Z	34.311	45.525	5	4.1	mb
2011-04-07T04:47:36.400Z	34.36	45.57	17.8	4.6	mb
2011-04-07T05:16:13.000Z	34.44	45.49	5	4.1	mblg
2011-04-08T04:27:44.800Z	34.457	45.462	24.5	4.1	mb
2011-11-29T07:58:15.900Z	34.76	45.23	16.2	4.3	mb
2013-10-14T20:33:19.440Z	34.7593	46.0454	11.95	4.2	mb
2013-11-05T04:03:39.600Z	34.896	45.083	9.5	4	mb
2013-11-22T06:51:25.060Z	34.4574	45.4824	6	5.6	mwb
2013-11-22T10:09:58.730Z	34.4284	45.3833	5.55	4.2	mb
2013-11-22T15:23:24.000Z	34.39	45.5	14	3.8	mb
2013-11-22T18:30:58.010Z	34.3083	45.6105	14	5.8	mww
2013-11-22T19:24:05.600Z	34.304	45.612	12.1	3.9	mb
2013-11-22T20:43:46.250Z	34.0056	45.6456	10.08	4.1	mb
2013-11-22T21:02:33.030Z	34.1896	45.5917	10.06	4.4	mb
2013-11-23T06:52:02.460Z	34.2649	45.5609	10.37	4.2	mb
2013-11-23T23:26:20.600Z	34.2291	45.6639	10.06	5.2	mb
2013-11-24T06:56:57.800Z	34.251	45.62	12	4.2	mb
2013-11-24T18:03:13.030Z	34.1438	45.6274	10.78	5	mb
2013-11-24T18:05:41.670Z	34.1765	45.6171	14	5.4	mwb
2013-11-25T02:01:57.900Z	34.29	45.49	17	4	mb
2013-12-10T16:33:09.590Z	34.1563	45.6089	23.06	4.1	mb
2016-03-19T05:05:46.340Z	34.5391	46.9167	10	4.4	mb
2016-06-22T21:05:43.300Z	34.819	45.299	12	4.1	mb
2016-08-10T04:55:06.300Z	35.351	46.3	10	4.3	mb
2017-03-11T10:33:41.850Z	34.806	46.7822	10	4.1	mb
2017-11-12T17:35:31.450Z	34.3719	45.6871	10	4.6	mb
2017-11-12T18:18:17.180Z	34.9109	45.9592	19	7.3	mww
2017-11-12T18:29:52.130Z	34.9224	45.5873	10	5.3	mb
2017-11-12T19:54:07.610Z	34.7577	45.5352	7.6	4.4	mb
2017-11-12T21:16:17.960Z	34.2152	45.6173	10	4	mb
2017-11-12T21:33:21.480Z	34.4891	45.8099	10	4.5	mb
2017-11-12T22:30:59.580Z	34.5305	45.7708	10	4.6	mb
2017-11-12T23:37:19.500Z	34.1325	45.7249	10	4	mb
2017-11-13T00:20:51.680Z	34.5466	45.8824	10	4.7	mb
2017-11-13T03:14:36.290Z	34.8864	45.8365	10	4.3	mb

2017-11-13T04:27:55.600Z	34.4217	45.7806	10	4.9	mb
2017-11-13T04:36:12.620Z	34.4089	45.7853	9.83	4.5	mb
2017-11-13T04:41:42.830Z	35.0671	45.8121	10	4.3	mb
2017-11-13T05:04:24.420Z	34.5897	45.8316	10	4.3	mb
2017-11-13T08:28:51.420Z	34.5686	45.5746	10.53	4.6	mb
2017-11-13T09:19:28.800Z	34.3482	45.7568	10	4.9	mb
2017-11-13T13:12:36.660Z	34.3018	45.7469	10	4.7	mb
2017-11-13T14:01:48.780Z	34.9133	45.8073	10	4.5	mb
2017-11-13T15:00:44.170Z	34.3179	45.5856	10	4.7	mb
2017-11-13T15:11:16.110Z	34.4729	45.8463	10	4.4	mb
2017-11-13T15:36:48.660Z	34.2831	45.7618	17.89	4.3	mb
2017-11-13T20:56:30.020Z	34.7299	45.5488	17.55	4.3	mb
2017-11-14T00:06:36.750Z	34.5723	45.4086	10	4.2	mb
2017-11-14T01:08:46.630Z	34.4473	45.7997	10	4.5	mb
2017-11-14T01:45:49.370Z	34.5058	45.7085	10	4.3	mb
2017-11-14T15:16:05.810Z	34.661	45.5937	16.3	4.4	mb
2017-11-15T07:11:21.210Z	34.559	45.8132	10	4	mb
2017-11-15T15:20:37.500Z	34.5781	45.6185	12	4.4	mb
2017-11-16T13:00:33.360Z	34.4586	45.9757	10	4.2	mb
2017-11-17T14:02:51.960Z	34.5301	45.5151	10	4.5	mb
2017-11-18T04:12:14.410Z	34.4657	45.6572	10	4.7	mb
2017-11-19T01:07:33.500Z	34.4024	45.8987	10	4.2	mb
2017-11-19T02:59:16.890Z	34.4863	45.9532	10	4.1	mb
2017-11-19T06:19:50.590Z	35.0332	46.2311	10	4.1	mb
2017-11-20T15:35:57.150Z	34.6696	45.8337	10	4.5	mb
2017-11-20T15:36:53.840Z	34.6412	45.7393	11.2	4.9	mb
2017-11-22T16:42:36.860Z	34.916	45.5326	10	4.2	mb
2017-11-22T19:47:13.630Z	34.7578	45.6647	10	4.3	mb
2017-11-22T20:34:03.910Z	34.7958	45.6562	10	4.2	mb
2017-11-26T05:47:30.370Z	34.4912	45.8072	10	4.6	mb
2017-11-27T03:00:28.980Z	34.8224	45.7052	10	4.4	mb
2017-12-01T19:27:08.810Z	34.3645	46.4377	10	4.3	mb
2017-12-01T20:17:06.980Z	34.3997	46.4431	10	4.5	mb
2017-12-06T05:53:42.450Z	34.9716	45.7893	10	4.8	mb
2017-12-06T07:57:40.350Z	34.54	45.7753	10	4.8	mb
2017-12-08T01:55:01.810Z	35.1223	45.7924	10	4.2	mb
2017-12-08T07:39:45.960Z	34.5187	45.7414	10	4.2	mb
2017-12-11T14:09:57.360Z	35.0786	45.7614	17.55	5.4	mww
2017-12-11T14:42:40.930Z	35.0283	45.7471	14.71	4.7	mb
2017-12-14T13:26:47.810Z	34.4534	45.4926	10	4.1	mb
2017-12-19T09:15:45.630Z	34.6946	45.7276	10	4.3	mb
2017-12-20T20:01:05.290Z	34.4279	45.7971	10	4.7	mb

2017-12-20T20:22:08.770Z	34.7662	46.1785	10	4.7	mb
2017-12-21T02:50:14.240Z	34.4989	45.8281	10	4.5	mb
2017-12-26T09:11:33.720Z	34.858	46.0246	10	4.5	mb
2017-12-26T15:32:59.380Z	34.8472	46.4693	10	4.6	mb
2018-01-05T06:32:56.820Z	34.5697	45.5827	10	4.3	mb
2018-01-06T15:22:09.120Z	34.5849	45.7696	10	5	mww
2018-01-07T02:01:46.400Z	34.5558	45.8285	10	4.2	mb
2018-01-10T15:56:28.980Z	34.6725	46.6764	10	4.6	mb
2018-01-18T16:48:38.450Z	34.4907	45.2213	10.43	4	mb
2018-01-21T02:19:37.010Z	34.5033	45.4454	10	4.2	mb
2018-01-21T05:45:39.890Z	34.6336	45.5972	10	4.1	mb
2018-01-25T03:19:13.940Z	34.658	46.2858	10	4	mb
2018-02-01T20:14:48.500Z	34.5902	45.4786	10	4.4	mb
2018-02-19T11:02:00.080Z	34.3132	45.3496	10	4.6	mb
2018-03-28T00:27:03.790Z	34.3702	45.4558	10	4.4	mb
2018-03-28T01:19:20.180Z	34.3729	45.4381	10	4.3	mb
2018-03-28T01:55:30.400Z	34.3755	45.5579	10	4.2	mb
2018-04-01T08:35:26.410Z	34.4028	45.7476	10	5	mww
2018-04-02T03:03:23.670Z	34.3435	45.782	10	4.2	mb
2018-05-22T00:31:53.210Z	34.8906	45.8006	10	4.5	mb
2018-05-22T00:35:58.490Z	34.8994	45.9697	17.11	4.3	mb
2018-06-06T00:07:08.310Z	34.557	46.1006	10	4	mb
2018-06-23T21:37:49.290Z	34.37	45.9165	10	4.3	mb
2018-06-26T17:57:04.640Z	34.6473	46.138	10	4.7	mb
2018-06-26T22:13:05.620Z	34.5339	45.6278	9.43	4.4	mb
2018-07-15T07:11:01.410Z	34.6386	46.2454	10	4.5	mb
2018-07-16T05:33:50.950Z	34.6339	46.4869	10	4.1	mb
2018-07-22T10:07:27.220Z	34.5909	46.1661	12	5.8	mww
2018-07-22T16:48:49.700Z	34.6191	46.2607	10	4.4	mb
2018-07-23T00:59:49.730Z	34.5567	46.2181	10	4.3	mb
2018-07-24T08:46:12.160Z	34.5762	46.2547	10	4.3	mb
2018-07-24T19:58:29.570Z	34.7438	45.5621	10	4.3	mb
2018-07-25T01:47:47.560Z	34.6291	46.3206	10	4.3	mb
2018-07-26T15:51:17.430Z	34.1817	45.6017	10	4.1	mb
2018-08-04T17:02:03.410Z	34.548	46.2323	26.49	4.1	mb
2018-08-25T22:13:25.620Z	34.6111	46.2422	10	6	mww
2018-08-25T22:40:37.050Z	34.6443	46.2561	10	4.3	mb
2018-08-25T23:25:05.840Z	34.5676	46.2361	10	4.4	mb
2018-08-26T00:53:53.980Z	34.7062	46.5108	10	4.3	mb
2018-08-26T05:18:27.910Z	34.5657	46.2057	10	4.2	mb
2018-08-26T08:25:03.190Z	34.6463	46.3395	10	4	mb
2018-08-26T09:23:33.250Z	34.5589	46.1467	10	4.5	mb

2018-08-26T15:51:41.750Z	34.619	46.1194	10	4.2	mb
2018-08-27T15:28:41.000Z	34.6959	46.2537	10	4.2	mb
2018-08-29T05:34:37.980Z	34.7682	46.1199	10	4.8	mb
2018-08-29T18:55:41.960Z	34.6434	46.231	10	4.1	mb
2018-08-31T21:05:44.360Z	34.6512	46.0736	10	5.3	mwr
2018-09-01T05:31:11.970Z	34.3868	45.7902	10	4.4	mb
2018-09-03T08:25:21.120Z	34.4606	45.4909	10	4.4	mb
2018-09-09T23:53:55.410Z	34.3659	45.8045	10	4.3	mb
2018-09-13T17:05:12.850Z	34.6984	45.9766	10	4.1	mb
2018-09-30T23:49:24.860Z	34.5376	46.2001	10	4.4	mb
2018-10-17T03:16:54.760Z	34.4333	45.4753	10	4.5	mb
2018-10-20T11:33:36.400Z	34.5944	46.127	10	4	mb
2018-11-05T20:32:09.530Z	34.6884	46.1554	10	4.2	mb
2018-11-17T19:19:06.090Z	34.5709	46.2268	10	4.5	mb
2018-11-19T22:37:44.010Z	34.612	46.0604	10	4.4	mb
2018-11-25T16:37:32.830Z	34.3609	45.7443	18	6.3	mww
2018-11-25T17:09:36.010Z	34.4157	45.7209	10	5.2	mww
2018-11-25T17:31:18.200Z	34.3095	45.7095	10	4.2	mb
2018-11-25T20:42:40.790Z	34.0887	45.6969	10	4.3	mb
2018-11-25T20:56:37.520Z	34.147	45.5038	10	4.5	mb
2018-11-25T22:28:20.130Z	34.2571	45.4842	10	4.4	mb
2018-11-25T23:00:46.470Z	34.238	45.6438	10	5	mb
2018-11-26T00:38:36.740Z	34.3869	45.7492	10	4.9	mb
2018-11-26T01:19:41.530Z	34.3065	45.6989	10	4.9	mb
2018-11-27T06:36:34.150Z	34.3789	45.4852	10	4.6	mb
2018-11-27T11:11:45.760Z	34.1276	45.6461	10	4.4	mb
2018-11-27T23:50:10.020Z	34.2214	45.6628	10	4.4	mb
2018-11-29T13:16:23.460Z	34.3993	45.8891	10	4.5	mb
2018-12-04T20:23:58.340Z	35.0228	46.6261	10	3.7	mb
2018-12-09T03:24:10.560Z	34.2797	45.8032	10	4.7	mb
2018-12-27T22:57:03.130Z	34.4699	45.6522	10	4.2	mb
2019-01-04T17:17:33.280Z	34.2672	45.7003	10.99	4.2	mb
2019-01-05T19:19:08.760Z	34.6268	46.2505	10	4.2	mb
2019-01-06T13:41:59.060Z	34.1248	45.6794	14	5.6	mww
2019-01-06T13:54:19.910Z	34.0932	45.5111	7.18	4.6	mb
2019-01-06T13:55:06.710Z	34.0765	45.5737	10	4.6	mb
2019-01-06T14:03:54.950Z	34.064	45.7651	10	4.2	mb
2019-01-06T14:15:07.940Z	34.0464	45.6698	10	4.9	mb
2019-01-06T14:29:26.230Z	34.2301	45.4634	10	4.1	mb
2019-01-14T18:17:59.700Z	34.1417	45.6339	10	4.3	mb
2019-01-15T17:07:00.410Z	34.0508	45.5913	10	4	mb
2019-01-29T05:18:23.770Z	34.4014	45.1199	10	4.3	mb

2019-02-07T05:37:14.950Z	34.1726	45.6014	10	4	mb
2019-02-21T09:01:36.720Z	34.775	46.0566	10	4.3	mb
2019-03-12T12:05:20.113Z	34.2825	45.5083	10	4.3	mb
2019-03-12T12:06:05.232Z	34.0432	45.425	10	4.5	mb
2019-04-15T06:34:32.944Z	34.5492	45.6064	10	4.4	mb
2019-05-11T10:28:59.929Z	34.9557	45.7333	10	5.2	mww
2019-05-25T18:26:41.112Z	34.8282	45.8045	10	4.2	mb
2019-06-05T03:33:05.508Z	34.369	45.6153	10	4.7	mb
2019-06-05T03:36:15.632Z	34.4738	45.7379	10	4.6	mb
2019-06-12T23:21:55.682Z	34.9344	46.482	10	4.1	mb
2019-06-23T16:51:59.868Z	34.4405	45.6199	10	4.7	mb
2019-07-17T15:19:32.703Z	34.3355	45.6504	10	4.5	mb
2019-07-29T20:47:09.847Z	34.3828	45.644	10	4.7	mb
2019-08-03T00:26:06.921Z	34.5931	46.2472	10	4.2	mb
2019-09-09T22:40:52.641Z	34.3387	45.6771	10	4.3	mb
2019-09-17T19:29:56.882Z	35.3483	46.2087	18.67	4.6	mb

S1. Thermo-Hydro-Mechanical Coupling Constitutive Equations

THM coupling theory was developed according to poro-elasticity and thermo-elasticity. Specifically, elastic deformation is described by Hooke's law, the fluid seepage in a porous medium by Darcy's law, and heat conduction by Fourier's law. These processes are coupled using the continuity equation and momentum conservation equation [2,3–5]. The following summarizes the physical equations.

S1.1. Poro-Elasticity Equations

Poro-elasticity is usually used to describe the interaction between fluid flow and the elastic deformation of porous media. Here, the constitutive equations were derived from Biot [3]:

$$\sigma = \sigma_{ex} + \mathbf{C}\varepsilon - \alpha_B p_f \mathbf{I}, \tag{S1}$$

where σ is the Cauchy stress tensor, ε is the elastic strain tensor, α_B is the Biot–Willis coefficient, p_f is the fluid pore pressure, $\mathbf{C}$ is the elastic tensor under drained and constant pore pressure, $\mathbf{I}$ is the characteristic tensor, and σ_{ex} indicates the contributions of pre-stress and viscoelastic stress. In this study, the Kelvin–Voigt viscoelastic model was used, and the viscous stress contribution was expressed as:

$$\sigma_{vis} = 2\eta\dot{\varepsilon} = 2G\tau\dot{\varepsilon}, \tag{S2}$$

where η is the viscosity coefficient, G is the shear modulus, and τ is the relaxation time.

According to Biot theory, fluid pressure is linear with the volumetric strain of porous media and the fluid increment, namely:

$$p_f = \frac{1}{S}(\varsigma - \alpha_B \varepsilon_{vol}), \tag{S3}$$

where ς is the fluid increment, ε_{vol} is the volumetric strain of the porous medium, and the water storage coefficient S can be expressed by the expression:

$$S = \frac{\varepsilon_p}{K_f} + (\alpha_B - \varepsilon_p)\frac{1-\alpha_B}{K_d}, \tag{S4}$$

where ε_p is the porosity, K_f is the fluid bulk modulus, and K_d is the volume modulus of the porous medium under drained conditions.

In the theoretical model of poro-elasticity, Darcy's law describes the flow of fluid in a porous media:

$$\mathbf{u} = -\frac{\kappa}{\mu}(\nabla p_{\mathrm{f}} + \rho_{\mathrm{f}} g \nabla D), \tag{S5}$$

According to the law of conservation of mass:

$$\frac{\partial}{\partial t}(\rho_{\mathrm{f}}\varepsilon_{\mathrm{f}}) + \nabla \cdot (\rho_{\mathrm{f}}\mathbf{u}) = Q_m, \tag{S6}$$

and the storage model:

$$\frac{\partial}{\partial t}(\rho_{\mathrm{f}}\varepsilon_{\mathrm{f}}) = \rho_{\mathrm{f}} S \frac{\partial p_{\mathrm{f}}}{\partial t}, \tag{S7}$$

Furthermore, the volume increase of fluid in the porous medium is equal to the volumetric compression of the pores:

$$Q_m = -\rho_{\mathrm{f}}\alpha_{\mathrm{B}}\frac{\partial}{\partial t}\varepsilon_{\mathrm{vol}}, \tag{S8}$$

Finally, we get the fluid continuity equation:

$$\rho_{\mathrm{f}} S \frac{\partial p_{\mathrm{f}}}{\partial t} + \nabla \cdot (\rho_{\mathrm{f}}\mathbf{u}) = -\rho_{\mathrm{f}}\alpha_{\mathrm{B}}\frac{\partial}{\partial t}\varepsilon_{\mathrm{vol}}, \tag{1}$$

where $\mathbf{u}$ is the Darcy velocity tensor, κ is the permeability of the porous medium, μ is the viscosity of the fluid, ∇p_f is the fluid pressure gradient, ρ_f is the fluid density, g is the acceleration due to gravity, and ∇D is the elevation gradient.

S1.2. Thermo-Elasticity Equations

Thermo-elasticity is usually used to describe the interaction between thermal energy and stress–strain. In this study, we mainly considered two heat transfer mechanisms—thermal convection and heat conduction—and one heat generation mechanism—deformation induced heating. The local heat balance theory was adopted; that is, the temperature difference between the rock mass and the fluid was not considered because this study focused on the evolution of total heat and did not specifically consider the heat in rocks or fluid [4,5].

The equations for thermal conservation including heat conduction and heat convection are given as:

$$\left(\rho C_p\right)_{\mathrm{eff}}\frac{\partial T}{\partial t} + \rho C_p \mathbf{u} \cdot \nabla T + \nabla \cdot \mathbf{q} = \mathrm{Q} + \mathrm{Q}_{\mathrm{ted}}, \tag{2}$$

$$\mathbf{q} = -k_{\mathrm{eff}}\nabla T, \tag{S9}$$

where $\left(\rho C_p\right)_{\mathrm{eff}}$ is the volume heat capacity at constant pressure, and can be expressed as:

$$\left(\rho C_p\right)_{\mathrm{eff}} = \theta_{\mathrm{p}}\rho_{\mathrm{p}}C_{p,\mathrm{p}} + \left(1-\theta_{\mathrm{p}}\right)\rho C_p, \tag{S10}$$

where ρ is the fluid density, C_p is the constant pressure heat capacity of the fluid, $C_{p,\mathrm{p}}$ is the heat capacity of a porous media at constant pressure, $\mathbf{q}$ is the conduction heat flux, $\mathbf{u}$ is the Darcy velocity, $\mathbf{Q}$ is the heat source or sink (not including radioactive and frictional heat), and k_{eff} is the effective heat conductive coefficient, which is determined by the thermal conductive coefficients of fluid k and porous media k_{p}, and the porosity θ_{p}:

$$k_{\mathrm{eff}} = \theta_{\mathrm{p}}k_{\mathrm{p}} + \left(1-\theta_{\mathrm{p}}\right)k, \tag{S11}$$

CT can be expressed by the enthalpy, $\boldsymbol{H}$:

$$\mathrm{CT} = \rho\mathbf{u}(\boldsymbol{H} - \frac{p}{\rho}), \tag{S12}$$

where $\boldsymbol{H}$ is expressed as:

$$\boldsymbol{H} = \int_{\mathbf{r_0}}^{\mathbf{r_1}} \boldsymbol{\nabla}_{\mathrm{r}}\boldsymbol{H}(\mathbf{r}) \cdot d\mathbf{r}, \tag{S13}$$

where **r** is the integration vector variable containing temperature and pressure components. The starting point, $\mathbf{r}_0$, is the value of **r** at reference conditions.

Table S2. Parameters of the thermo-hydro-mechanical (THM) coupled model.

Mechanical Parameter		Hydraulic Parameters		Thermal Parameters	
Young's modulus, E (Pa)	4×10^{10}–6×10^{10}	Porosity, θ	0.02	Heat capacity of rock at constant pressure, $C_{p,p}$ [J/(kg·K)]	850
Poisson's ratio, ν	0.25	Permeability, κ (m^2)	1×10^{-16}	Heat capacity of water at constant pressure, C_p [J/(kg·K)]	2400
Density, ϱ (kg/m^3)	2500–3000	Dynamic viscosity, μ (Pa·s)	8.8×10^{-4}	Rock thermal expansion coefficient, α (1×10^{-6}/K)	2.20
		Biot–Willis coefficient, α_B	0.47	Water thermal expansion coefficient, α (1×10^{-5}/K)	2.72–17.1
		Water density, ϱ (kg/m^3)	1000	Reference temperature, T_{ref} (K)	290.78

S2. Significance Test Methods

S2.1. Mann-Kendall Trend Test

Testing trends was done at the specific α significance level. When $|Z_S| > Z_{1-\alpha/2}$, the null hypothesis is rejected and a significant trend exists in the time series. In this study, significance level $\alpha = 0.05$ was used, and the null hypothesis of no trend is rejected if $|Z_S| > 1.96$ [6–8].

S2.2. Sen's Slope

The confidence interval of $\alpha = 0.05$ was computed as follows:

$$C_\alpha = Z_{1-\alpha/2}\sqrt{Var(S)}, \tag{S14}$$

$$M_1 = \frac{N - C_\alpha}{2}, \tag{S15}$$

$$M_2 = \frac{N + C_\alpha}{2}, \tag{S16}$$

The lower and upper limits of the confidence interval are the M_1th largest and the (M_2 + 1)th largest of the N ordered slope estimates [7,9].

Table S3. Historical and post-seismic k time series trends [1].

Areas	Time	Reg. (h/d)	95% Confidence Interval		Zs	5% Significance Level	Q_{med}	95% Confidence Interval	
WA1	2010	−0.056	−0.189	0.077	−1.001	1.960	−0.090	−0.275	0.087
	2011	−0.091	−1.499	1.317	/	/	/	/	/
	2012	−0.081	−0.551	0.389	−0.109	1.960	−0.079	−1.149	0.747
	2013	−0.273	−0.869	0.323	−1.166	1.960	−0.571	−1.528	0.559
	2014	−0.166	−0.260	−0.072	−1.868	1.960	−0.545	−0.927	0.014
	2015	−0.105	−0.279	0.068	−0.766	1.960	−0.125	−0.370	0.208
	2016	−0.610	−1.213	−0.007	−2.147	1.960	−0.602	−2.023	−0.025
	2017	−0.213	−0.393	−0.034	−1.166	1.960	−0.270	−0.902	0.257
WA2	2010	−0.041	−0.107	0.026	−1.056	1.960	−0.061	−0.137	0.079
	2011	−0.062	−0.138	0.014	−1.361	1.960	−0.336	−0.638	0.034
	2012	−0.033	−0.319	0.254	−0.313	1.960	−0.184	−1.529	0.428
	2013	−0.319	−1.657	1.019	/	/	/	/	1.263
	2014	−0.138	−0.406	0.129	−0.730	1.960	−0.400	−1.450	0.222
	2015 [2]	0.096	−0.049	0.24	1.147	1.96	0.256	−0.234	0.399
	2016	−0.454	−0.976	0.069	−2.949	1.960	−0.307	−0.586	−0.057
	2017	−0.067	−0.264	0.130	−0.343	1.960	−0.060	−0.716	0.215
WA3	2010	−0.072	−0.239	0.095	−1.067	1.960	−0.104	−0.288	0.027
	2011	−0.094	−0.213	0.024	−0.938	1.960	−0.036	−0.860	0.065
	2012	−0.426	−0.615	−0.237	−2.398	1.960	−1.134	−1.731	−0.120
	2013	−0.617	−1.701	0.466	/	/	/	/	−0.254
	2014	−0.183	−0.358	−0.008	−0.915	1.960	−0.214	−0.941	0.508
	2015 [2]	0.167	−0.057	0.391	2.189	1.96	0.292	0.16	0.242
	2016	−0.601	−0.893	−0.310	−2.623	1.960	−0.832	−1.462	−0.249
	2017	−0.209	−0.402	−0.015	−1.769	1.960	−0.200	−0.584	−0.036
CA1	2010	−0.023	−0.123	0.077	−0.687	1.960	−0.046	−0.215	0.100
	2011	−0.100	−0.251	0.051	−0.226	1.960	−0.010	−0.171	0.110
	2012	−0.249	−0.631	0.133	/	/	/	/	/
	2013	−0.279	−1.044	0.485	/	/	/	/	/
	2014	−0.105	−0.646	0.436	−1.166	1.960	−0.267	−1.612	0.585
	2015	−0.018	−0.186	0.151	−0.865	1.960	−0.102	−0.396	0.277
	2016	−0.517	−1.036	0.001	−2.239	1.960	−0.353	−0.741	−0.043
	2017	0.172	−0.148	0.492	0.530	1.960	0.085	−0.248	0.430
CA2	2010	0.019	−0.153	0.191	−0.350	1.960	−0.029	−0.170	0.103

2011	−0.459	−0.783	−0.135	−1.136	1.960		−0.104	−0.307	0.115
2012	−0.173	−0.635	0.288	−0.938	1.960		−0.594	−2.610	0.419
2013	−0.163	−1.220	0.895	/	/		/	/	/
2014	−0.394	−0.756	−0.033	−1.557	1.960		−1.192	−2.646	0.565
2015	−0.126	−0.321	0.070	−0.617	1.960		−0.218	−0.743	0.164
2016	−0.170	−0.358	0.018	−1.756	1.960		−0.225	−0.382	0.010
2017	−0.040	−0.183	0.102	0.000	1.960		0.000	−0.311	0.354

Notes: 1. WA, warming area; CA, cooling area; Reg., regression coefficient in hours per day (h/d); Zs, Mann-Kendall trend; Q_{med}, median of Sen's slope. 2. insufficient data could lead to abnormal k trends in 2015 (Table S4).

Table S4. Available k of WA2 and WA3 in 2015

Time	k in WA2	k in WA3
2015-11-12	1.649	3.614
2015-11-13	3.319	4.200
2015-11-14	3.042	6.637
2015-11-20	4.305	7.030
2015-11-21	4.134	4.680
2015-11-22	3.900	7.456
2015-11-23	5.029	7.810
2015-11-24	4.441	8.088
2015-11-28	2.769	5.594

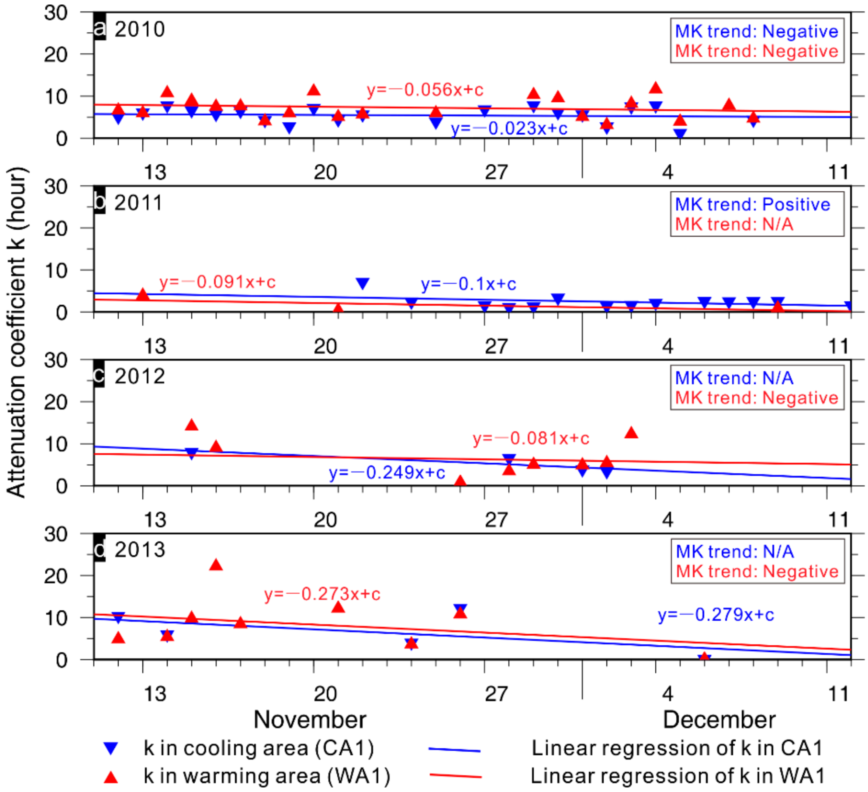

Figure S1. Historical k time series trends during (**a**) 2010, (**b**) 2011, (**c**) 2012; (**d**) 2013. Blue triangles denote k in the cooling area (CA1) and blue lines denote the linear regression through the data. Red triangles denote k in the warming area (WA1) and red lines denote the linear regression through the data. Regression coefficients are given in unit of hours per day (h/d). MK, Mann-Kendall.

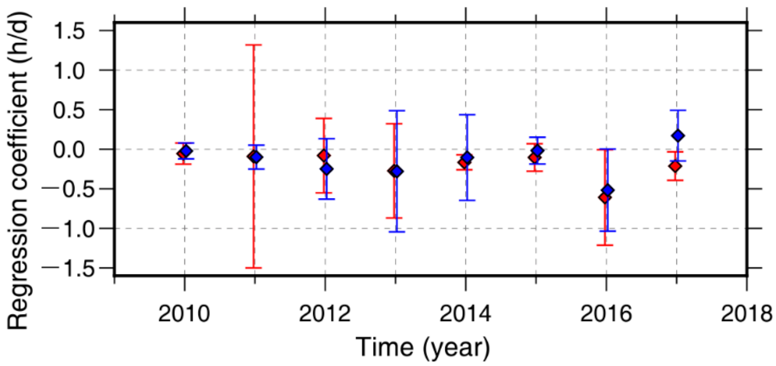

Figure S2. Regression coefficients and confidence interval of k time series during 2010 to 2017. Red diamonds and error bars indicate the regression coefficients and confidence intervals of WA1 warming zone respectively, and blue ones indicate those of CA1.

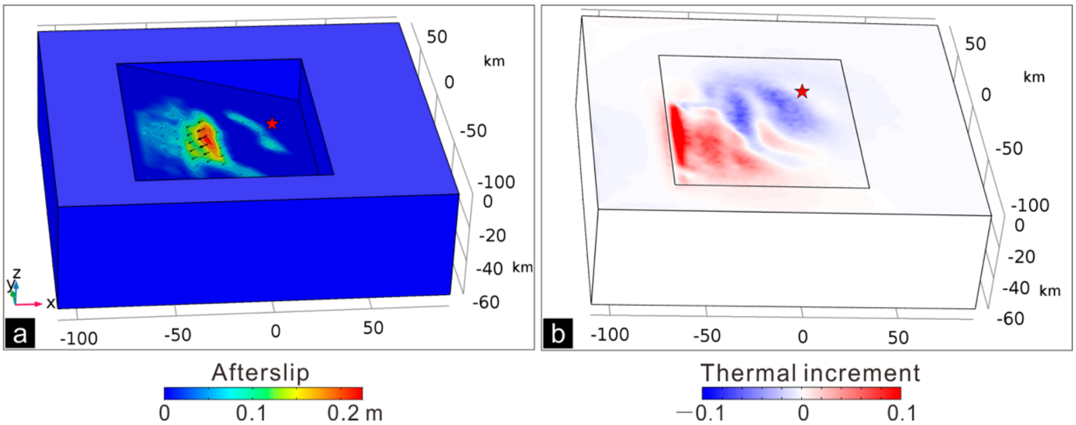

Figure S3. (**a**) Afterslip on the fault of the 2017 Iran earthquake and the geometric model. Red star denotes the United States Geological Survey (USGS) source position on the fault [1]. (**b**) Thermal increment at the surface caused by afterslip. Warm colors indicate warming and cool colors indicate cooling; the red star denotes the USGS epicenter on the surface.

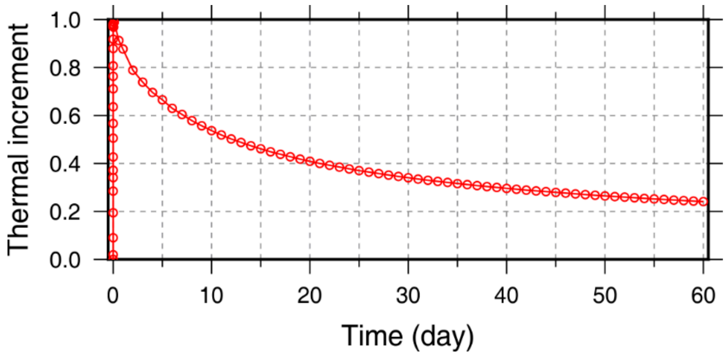

Figure S4. Evolution of post-seismic thermal increment at the center of WA1. Red circles represent the time steps of calculation. 0 represents the origin time of the 2017 Iran earthquake.

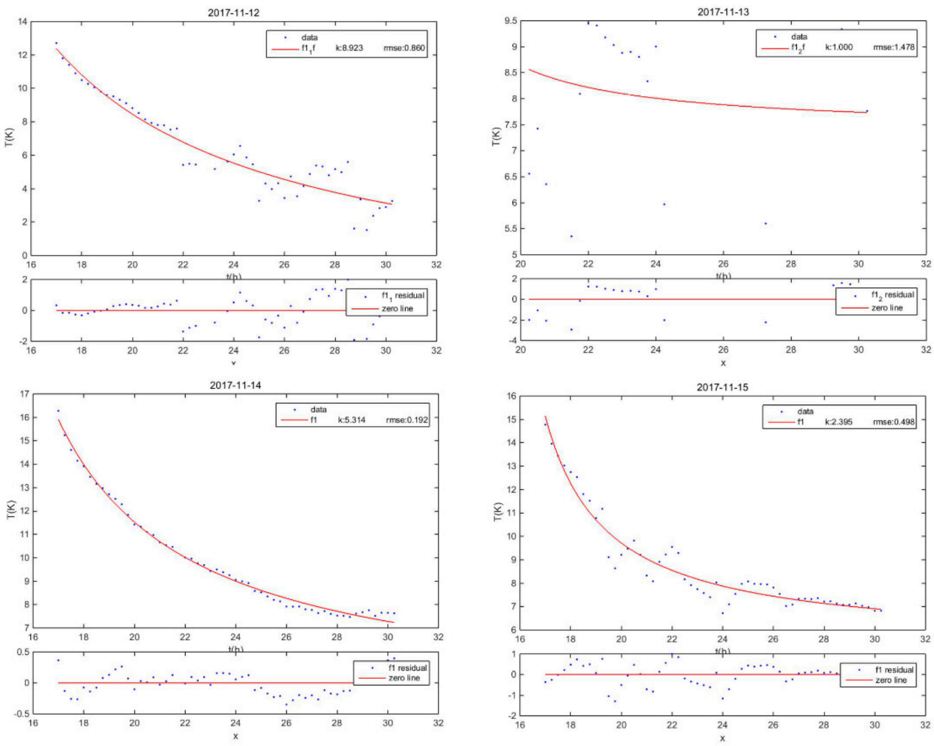

Figure S5. Comparison of fitting results of CA1 in 2017.

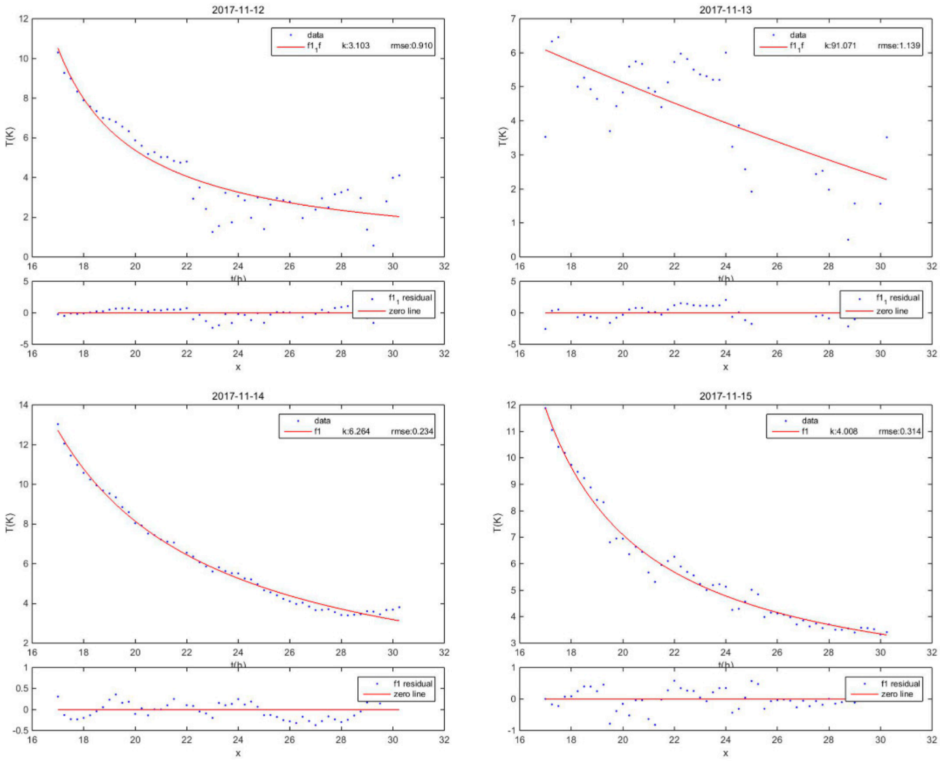

Figure S6. Comparison of fitting results of WA1 in 2017.

References

1. United States Geological Survey. Available online: https://www.usgs.gov/ (accessed on 4 September 2019).
2. Jing, L.; Feng, X. Numerical modeling for coupled thermo-hydro-mechanical and chemical processes (thmc) of geological media—International and Chinese experiences. *Chin. J. Rock Mech. Eng*. **2003**, *22*, 125–136.
3. Biot, M.A. Mechanics of Deformation and Acoustic Propagation in Porous Media. *J. Appl. Phys.* **1962**, *33*, 1482–1498.
4. Bear, J.; Bachmat, Y. Introduction to Modeling of Transport Phenomena in Porous Media. *Theory Appl. Trans. Porous Media* **1990**, *4*, 481–516.
5. Nield, D.A.; Bejan, A. *Convection in Porous Media*; Springer: Berlin, Germany, 2013; Volume 108, pp. 284–290.
6. Gocic, M.; Trajkovic, S. Analysis of changes in meteorological variables using Mann-Kendall and Sen's slope estimator statistical tests in Serbia. *Glob. Planet. Chang.* **2013**, *100*, 172–182.
7. Mann, H.B. Nonparametric tests against trend. *Econometrica* **1945**, *13*, 245–259.
8. Kendall, K. Thin-film peeling-the elastic term. *J. Phys. D* **1975**, *8*, 1449.
9. Gilbert, R.O. *Statistical Methods for Environmental Pollution Monitoring,* 1st ed.; John Wiley & Sons: New York, NY, USA, 1987; pp. 230–236.